Resolved and sub-grid-scale transport in CAM5-FV

Peter Hjort Lauritzen and Julio Bacmeister

Atmospheric Modeling and Predictability Section (AMP)
Climate and Global Dynamics Division (CGD)
NCAR Earth System Laboratory (NESL)
National Center for Atmospheric Research (NCAR)

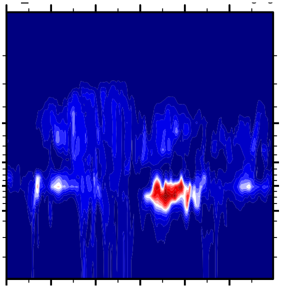

ACD group meeting

Motivation

Sometime in May Steven Massie and William Randel came into my visitor office in ACD and asked me: 'How do tracers get moved around in CAM?'

This Monday Laura Pan said: 'I have a lot of questions regarding how convection is represented in models like CAM/WACCM?'

The question I am going to address:

If you add a tracer to CAM-FV (with CAM5 physics), how is it 'moved around' both grid-scale and sub-grid-scale?

Physical processes on tracers

- 'Resolved' scale transport (Lin and Rood, 1996)
- Deep convective transport (Zhang and McFarlane, 1995; Neale et al., 2008)
- Shallow convective transport (Park and Bretherton, 2009)
- Turbulent transport (Park and Bretherton, 2009)
- Scavenging through wet deposition (only for aerosols not trace gases)
- Chemistry (for reactive tracers)

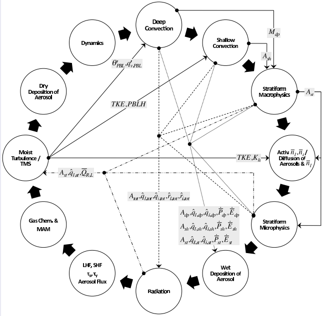

Figure from Park et al. (2012) - process split advancement of tendencies

Vertical coordinate

- CAM-FV uses a Lagrangian ('floating') vertical coordinate ξ so that

$$\frac{d\xi}{dt} = 0,$$

i.e. vertical surfaces are material surfaces (no flow across them).

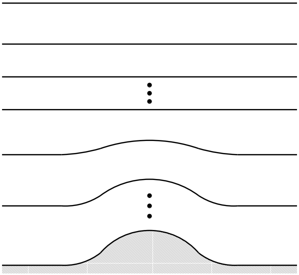

Figure shows 'usual' hybrid $\sigma - p$ vertical coordinate $\eta(p_s, p)$ (where p_s is surface pressure):

- $\eta(p_s, p)$ is a monotonic function of p.
- $\eta(p_s, p_s) = 1$
- $\eta(p_s, 0) = 0$
- $\eta(p_s, p_{top}) = \eta_{top}$.

Boundary conditions are:

- $\frac{d\eta(p_s, p_s)}{dt} = 0$
- $\frac{d\eta(p_s, p_{top})}{dt} = \omega(p_{top}) = 0$

Vertical coordinate

- CAM-FV uses a Lagrangian ('floating') vertical coordinate ξ so that

$$\frac{d\xi}{dt} = 0,$$

i.e. vertical surfaces are material surfaces (no flow across them).

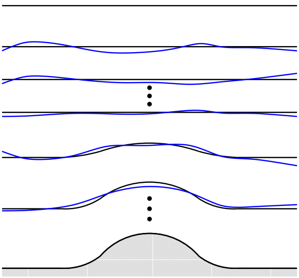

Figure:

- Set $\xi = \eta$ at time t_{start} (black lines).
- For $t > t_{start}$ the vertical levels deform as they move with the flow (blue lines).
- To avoid excessive deformation of the vertical levels (non-uniform vertical resolution) the prognostic variables defined in the Lagrangian layers ξ are periodically remapped (= conservative interpolation) back to the Eulerian reference coordinates η (more on this later).

Adiabatic frictionless equations of motion using Lagrangian vertical coordinates

Assuming a Lagrangian vertical coordinate the hydrostatic equations of motion integrated over a layer can be written as

$$
\begin{aligned}
\text{mass air:} \quad & \frac{\partial(\delta p)}{\partial t} = -\nabla_h \cdot (\vec{v}_h \delta p)\,, \\
\text{mass tracers:} \quad & \frac{\partial(\delta p q)}{\partial t} = -\nabla_h \cdot (\vec{v}_h\, q \delta p)\,, \\
\text{horizontal momentum:} \quad & \frac{\partial \vec{v}_h}{\partial t} = -\left(\zeta + f\right) \vec{k} \times \vec{v}_h - \nabla_h \kappa - \nabla_p \Phi, \\
\text{thermodynamic:} \quad & \frac{\partial(\delta p \Theta)}{\partial t} = -\nabla_h \cdot (\vec{v}_h \delta p \Theta)
\end{aligned}
$$

where δp is the layer thickness, $\vec{v}_h$ is horizontal wind, q tracer mixing ratio, ζ vorticity, f Coriolis, κ kinetic energy, Θ potential temperature. The momentum equations are written in vector invariant form.

Adiabatic frictionless equations of motion using Lagrangian vertical coordinates

Assuming a Lagrangian vertical coordinate the hydrostatic equations of motion integrated over a layer can be written as

$$
\begin{aligned}
\text{mass air:} \quad & \frac{\partial(\delta p)}{\partial t} = -\nabla_h \cdot (\vec{v}_h \delta p)\,, \\
\text{mass tracers:} \quad & \frac{\partial(\delta p q)}{\partial t} = -\nabla_h \cdot (\vec{v}_h\, q \delta p)\,, \\
\text{horizontal momentum:} \quad & \frac{\partial \vec{v}_h}{\partial t} = -(\zeta + f)\,\vec{k} \times \vec{v}_h - \nabla_h \kappa - \nabla_p \Phi, \\
\text{thermodynamic:} \quad & \frac{\partial(\delta p \Theta)}{\partial t} = -\nabla_h \cdot (\vec{v}_h \delta p \Theta)
\end{aligned}
$$

The equations of motion are discretized using an Eulerian finite-volume approach.

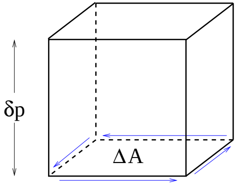

Integrate the flux-form continuity equation horizontally over a control volume:

$$\frac{\partial}{\partial t}\iint_A \delta p \, dA = -\iint_A \nabla_h \left(\vec{v}_h \delta p\right) \, dA, \tag{1}$$

where A is the horizontal extent of the control volume. Using Gauss's divergence theorem for the right-hand side of (1) we get:

$$\frac{\partial}{\partial t}\iint_A \delta p \, dA = -\oint_{\partial A} \delta p \, \vec{v} \cdot \vec{n} \, dA, \tag{2}$$

where ∂A is the boundary of A and $\vec{n}$ is outward pointing normal unit vector of ∂A.

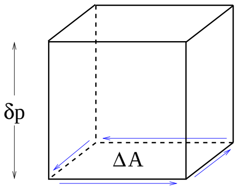

Integrate the flux-form continuity equation horizontally over a control volume:

$$\frac{\partial}{\partial t}\iint_A \delta p \, dA = -\iint_A \nabla_h \left(\vec{v}_h \delta p\right) \, dA, \tag{1}$$

where A is the horizontal extent of the control volume. Using Gauss's divergence theorem for the right-hand side of (1) we get:

$$\frac{\partial}{\partial t}\iint_A \delta p \, dA = -\oint_{\partial A} \delta p \, \vec{v} \cdot \vec{n} \, dA, \tag{2}$$

Right-hand side of (2) represents the instantaneous flux of mass through the vertical faces of the control volume.

Finite-volume discretization of continuity equation

$$\frac{\partial}{\partial t} \iint_A \delta p \, dA = - \oint_{\partial A} \delta p \, \vec{v} \cdot \vec{n} \, dA. \tag{3}$$

Discretize (3) in space

$$\Delta A \, \frac{\partial \overline{\delta p}}{\partial t} = - \sum_{f=1}^{4} \left[\langle \delta p \vec{v} \rangle \cdot \vec{n} \Delta \ell \right]_f , \tag{4}$$

where

- $\overline{\delta} p$ = horizontal mean value of δp
- $\vec{n}_f$ = unit vector normal to the fth cell face pointing outward
- $\Delta \ell_f$ is the length of the face in question
- $\vec{v}_f$ = instantaneous values of $\vec{v}$ at the cell face f
- brackets represent averages in either λ or θ direction over the cell face.

Finite-volume discretization of continuity equation

$$\frac{\partial}{\partial t}\iint_A \delta p \, dA = -\oint_{\partial A} \delta p \, \vec{v}\cdot\vec{n}\, dA. \qquad (3)$$

Discretize (3) in space

$$\Delta A \frac{\partial \overline{\delta p}}{\partial t} = -\sum_{f=1}^{4}\left[\langle \delta p \vec{v}\rangle \cdot \vec{n}\Delta\ell\right]_f , \qquad (4)$$

and integrate (4) over the time-step Δt_{dyn}

$$\Delta A\, \overline{\delta p}^{n+1} = \Delta A\, \overline{\delta p}^{n} - \Delta t_{dyn} \sum_{f=1}^{4}\left[\overline{\overline{\langle \delta p \vec{v}\rangle}} \cdot \vec{n}\Delta\ell\right]_f , \qquad (5)$$

where n is the time-level index and the double-bar refers to the time average over Δt_{dyn}.

Each term in the sum on the right-hand side of (6) represents the mass transported through one of the four vertical control volume faces into the cell during one time-step (graphical illustration on next page).

Finite-volume discretization of continuity equation: Tracking mass

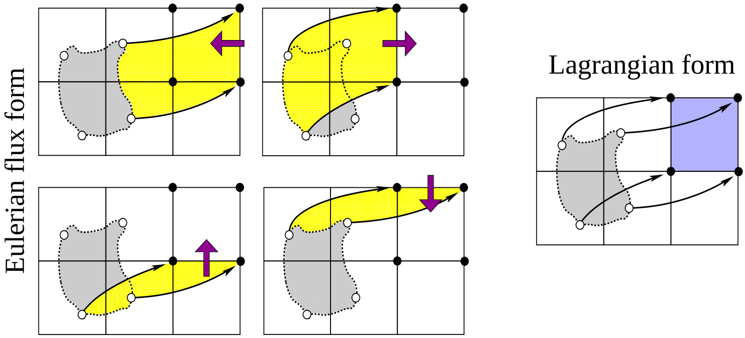

The yellow areas are ‘swept’ through the control volume faces during one time-step. The grey area is the corresponding Lagrangian area (area moving with the flow with no flow through its boundaries that ends up at the Eulerian control volume after one time-step). Black arrows show parcel trajectories.

Equivalence between Eulerian flux-form and Lagrangian form!

Finite-volume discretization of continuity equation: Tracking mass

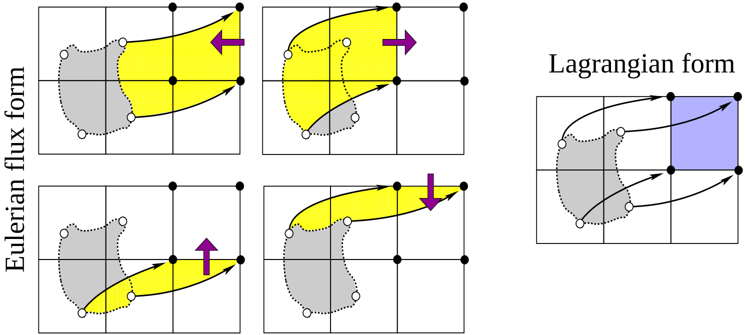

Until now everything has been exact. How do we approximate the fluxes numerically?

- In CAM-FV the Lin and Rood (1996) scheme is used which is a dimensionally split scheme (that is, rather than estimating the boundaries of the yellow areas and integrate over them, fluxes are estimated by successive applications of one-dimensional operators in each coordinate direction).

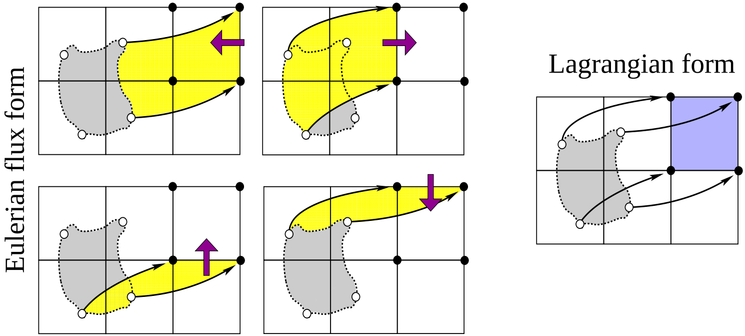

Until now everything has been exact. How do we approximate the fluxes numerically?

- (before showing equations for Lin and Rood (1996) scheme) What is the effective Lagrangian area associated with the Lin and Rood (1996) scheme?

Finite-volume discretization of continuity equation: Tracking mass

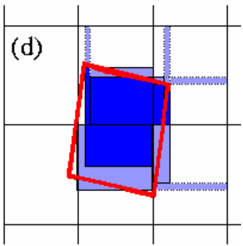

Figure: Red lines define boundary of exact Lagrangian cell for a special case with deformational, rotational and divergent wind field. Blue colors is Lagrangian cell associated with the Lin and Rood (1996) scheme. Dark blue shading weights integrated mass with 1 and light blue shading weights integrated mass with 1/2. See Machenhauer et al. (2009) for details.

Until now everything has been exact. How do we approximate the fluxes numerically?

- (before showing equations for Lin and Rood (1996) scheme) What is the effective Lagrangian area associated with the Lin and Rood (1996) scheme?

$$\boxed{\overline{\delta p}^{n+1} = \overline{\delta p}^{n} + F^{\lambda}\left[\frac{1}{2}\left(\overline{\delta p}^{n} + f^{\theta}(\overline{\delta p}^{n})\right)\right] + F^{\theta}\left[\frac{1}{2}\left(\overline{\delta p}^{n} + f^{\lambda}(\overline{\delta p}^{n})\right)\right],}$$

where

$$\begin{aligned} F^{\lambda,\theta} &= \text{ flux divergence in } \lambda \text{ or } \theta \text{ coordinate direction} \\ f^{\lambda,\theta} &= \text{ advective update in } \lambda \text{ or } \theta \text{ coordinate direction} \end{aligned}$$

The Lin and Rood (1996) advection scheme

$$\boxed{\overline{\delta p}^{n+1} = \overline{\delta p}^{n} + F^{\lambda}\left[\frac{1}{2}\left(\overline{\delta p}^{n} + f^{\theta}(\overline{\delta p}^{n})\right)\right] + F^{\theta}\left[\frac{1}{2}\left(\overline{\delta p}^{n} + f^{\lambda}(\overline{\delta p}^{n})\right)\right],}$$

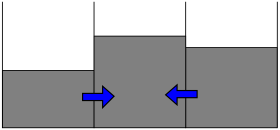

- Figure: Graphical illustration of flux-divergence operator F^{λ}. Shaded areas show cell average values for the cell we wish to make a forecast for and the two adjacent cells.

$$\boxed{\overline{\delta p}^{n+1} = \overline{\delta p}^{n} + F^{\lambda}\left[\frac{1}{2}\left(\overline{\delta p}^{n} + f^{\theta}(\overline{\delta p}^{n})\right)\right] + F^{\theta}\left[\frac{1}{2}\left(\overline{\delta p}^{n} + f^{\lambda}(\overline{\delta p}^{n})\right)\right],}$$

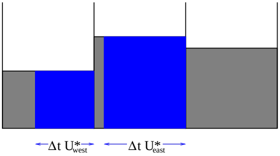

- $u^{*}_{east/west}$ are the time-averaged winds on each face (more on how these are obtained later).
- F^{λ} is proportional to the difference between mass 'swept' through east and west cell face.
- $f^{\lambda} = F^{\lambda} + \overline{\overline{<\delta p>}}\Delta t_{dyn} D$, where D is divergence.
- On Figure we assume constant sub-grid-cell reconstructions for the fluxes.

$$\boxed{\overline{\delta p}^{n+1} = \overline{\delta p}^{n} + F^{\lambda}\left[\frac{1}{2}\left(\overline{\delta p}^{n} + f^{\theta}(\overline{\delta p}^{n})\right)\right] + F^{\theta}\left[\frac{1}{2}\left(\overline{\delta p}^{n} + f^{\lambda}(\overline{\delta p}^{n})\right)\right],}$$

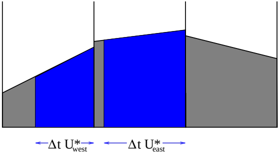

Higher-order approximation to the fluxes:

- Piecewise linear sub-grid-scale reconstruction (van Leer, 1977): Fit a linear function using neighboring grid-cell average values with mass-conservation as a constraint (i.e. area under linear function = cell average.).

$$\overline{\delta p}^{n+1} = \overline{\delta p}^{n} + F^{\lambda}\left[\frac{1}{2}\left(\overline{\delta p}^{n} + f^{\theta}(\overline{\delta p}^{n})\right)\right] + F^{\theta}\left[\frac{1}{2}\left(\overline{\delta p}^{n} + f^{\lambda}(\overline{\delta p}^{n})\right)\right],$$

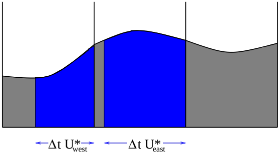

Higher-order approximation to the fluxes:

- Piecewise linear sub-grid-scale reconstruction (van Leer, 1977): Fit a linear function using neighboring grid-cell average values with mass-conservation as a constraint (i.e. area under linear function = cell average.).
- Piecewise parabolic sub-grid-scale reconstruction (Colella and Woodward, 1984): Fit parabola using neighboring grid-cell average values with mass-conservation as a constraint. Note: Reconstruction is C^0 across cell edges.

$$\overline{\delta p}^{n+1} = \overline{\delta p}^{n} + F^{\lambda}\left[\frac{1}{2}\left(\overline{\delta p}^{n} + f^{\theta}(\overline{\delta p}^{n})\right)\right] + F^{\theta}\left[\frac{1}{2}\left(\overline{\delta p}^{n} + f^{\lambda}(\overline{\delta p}^{n})\right)\right],$$

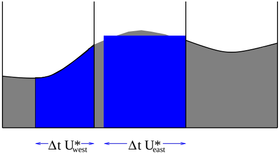

Higher-order approximation to the fluxes:

- Piecewise linear sub-grid-scale reconstruction (van Leer, 1977): Fit a linear function using neighboring grid-cell average values with mass-conservation as a constraint (i.e. area under linear function = cell average.).
- Piecewise parabolic sub-grid-scale reconstruction (Colella and Woodward, 1984): Fit parabola using neighboring grid-cell average values with mass-conservation as a constraint. Note: Reconstruction is continuous at cell edges.
- Reconstruction function may 'over'- or 'undershoot' which may lead to unphysical and/or oscillatory solutions. Use limiters to render reconstruction function shape-preserving.

The Lin and Rood (1996) advection scheme

$$\boxed{\overline{\delta p}^{n+1} = \overline{\delta p}^{n} + F^{\lambda}\left[\frac{1}{2}\left(\overline{\delta p}^{n} + f^{\theta}(\overline{\delta p}^{n})\right)\right] + F^{\theta}\left[\frac{1}{2}\left(\overline{\delta p}^{n} + f^{\lambda}(\overline{\delta p}^{n})\right)\right],}$$

Advantages:

- Inherently mass conservative (note: conservation does not necessarily imply accuracy!).
- Formulated in terms of one-dimensional operators.
- Preserves a constant for a non-divergent flow field (if the finite-difference approximation to divergence is zero).
- Preserves linear correlations between trace species (if shape-preservation filters are not applied)
- Has shape-preserving options. Note: Since the Lin and Rood (1996) is dimensionally split and the shape-preserving filters are applied along the coordinate axis tiny over-/under-shoot may be present in the traverse direction.

Free-stream preserving 'super-cycling' of tracers with respect to air ρ

Simply solving the tracer continuity equation for $\overline{q\delta p}^{n+1}$ using Δt_{trac} will lead to inconsistencies. Why?

Continuity equation for air δp

$$\frac{\partial \delta p}{\partial t} + \nabla \cdot (\delta p \, \vec{v}_h) = 0, \tag{6}$$

and a tracer with mixing ratio q

$$\frac{\partial (\delta p \, q)}{\partial t} + \nabla \cdot (\delta p \, q \, \vec{v}_h) = 0, \tag{7}$$

For $q = 1$ equation (7) reduces to (6). If this is satisfied in the numerical discretizations, the scheme is 'free-stream' preserving.

Solving (7) with $q = 1$ using Δt_{trac} will NOT produce the same solution as solving (6) `nspltrac` times using Δt_{dyn}!

Graphical illustration of 'free stream' preserving transport of tracers

Assume no flux through east cell wall.

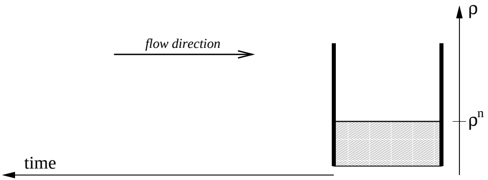

- Solve continuity equation for air $\rho = \delta p$ together with momentum and thermodynamics equations.

Graphical illustration of ‘free stream’ preserving transport of tracers

Assume no flux through east cell wall.

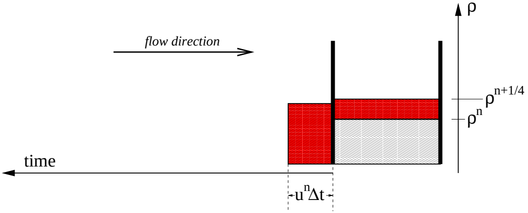

- Solve continuity equation for air $\rho = \delta p$ together with momentum and thermodynamics equations.

Graphical illustration of 'free stream' preserving transport of tracers

Assume no flux through east cell wall.

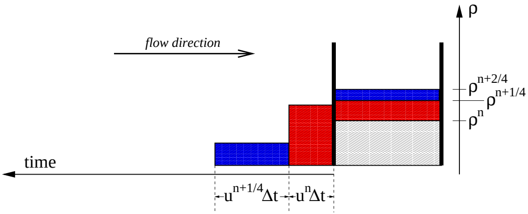

- Solve continuity equation for air $\rho = \delta p$ together with momentum and thermodynamics equations.
- Repeat *ksplit* times

Graphical illustration of ‘free stream’ preserving transport of tracers

Assume no flux through east cell wall.

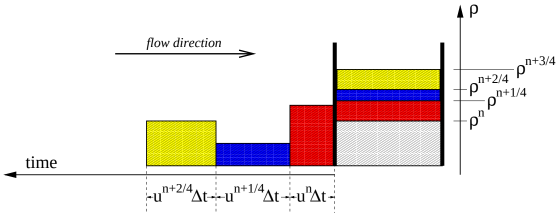

- Solve continuity equation for air $\rho = \delta p$ together with momentum and thermodynamics equations.
- Repeat *ksplit* times

Graphical illustration of 'free stream' preserving transport of tracers

Assume no flux through east cell wall.

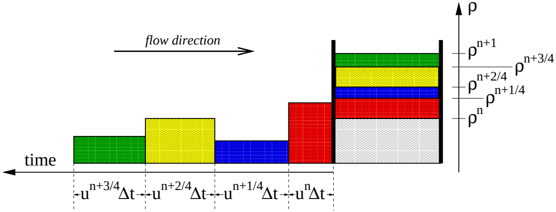

- Solve continuity equation for air $\rho = \delta p$ together with momentum and thermodynamics equations.
- Repeat *ksplit* times

Graphical illustration of 'free stream' preserving transport of tracers

Assume no flux through east cell wall.

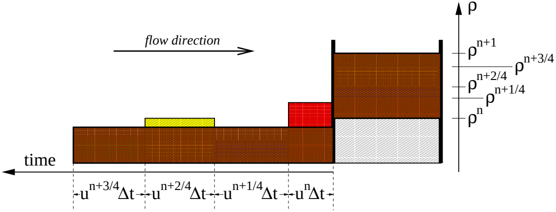

- Solve continuity equation for air $\rho = \delta p$ together with momentum and thermodynamics equations.
- Repeat *ksplit* times
- Brown area $=$ average flow of mass through cell face.
- Compute time-averaged value of q across brown area using Lin and Rood (1996) scheme: $\overline{\overline{<q>}}$.
- Forecast for tracer is: $\overline{\overline{<q>}} \times \sum_{i=1}^{ksplit} \delta p^{n+i/ksplit}$
- Yields 'free stream' preserving solution!

'Resolved' scale transport: FYI

We are 'switching' dynamical core

November release of CESM → CAM-SE (Spectral Elements)

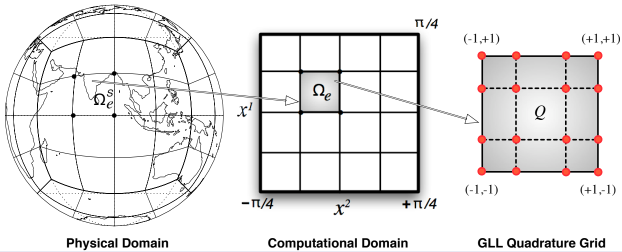

Fig. 9.22 A schematic diagram showing the mapping between each spherical tile (element) Ω_e^S of the physical domain (cubed-sphere) $\mathscr{S}$ onto a planar element Ω_e on the computational domain $\mathscr{C}$ (cube). For a DG discretization each element on the cube is further mapped onto a unique reference element Q, which is defined by the Gauss-Lobatto-Legendre (GLL) quadrature points. The horizontal discretization of the HOMME dynamical cores relies on this grid system.

Figure from Nair et al. (2011)

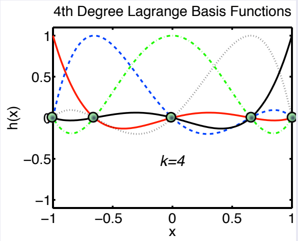

In default CAM-SE $n = 3$ (polynomials of degree 3; 4^{th}-order accurate)

Note: On Figure $n = 4$

Aside: Ongoing DOE project (PI: J.-F. Lamarque)

Among goals: Evaluate CAM-SE as a transport model (Lauritzen and Thuburn, 2012; Lauritzen et al., 2012), add specified dynamics option to CAM-SE and investigate higher-order dynamics-chemistry coupling.

Assesing 'accuracy' of tracer transport (Rasch et al., 2006)

Test case setup by Rasch et al. (2006) designed to assess transport in region of atmosphere

- (LOW) strongly influenced by sub-grid scale transport processes (convection and boundary layer processes),
- (HIGH) less strongly influenced by sub-grid scale processes; large role being played by resolved scale dynamics
- (MID) 'in the middle'!

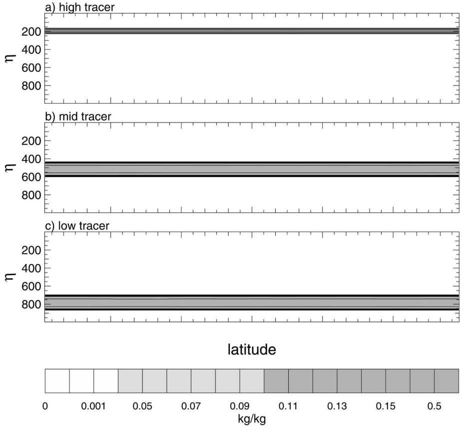

FIG. 1. Initial conditions for (a) HIGH, (b) MID, and (c) LOW tracer.

Assesing 'accuracy' of tracer transport (Rasch et al., 2006)

LOW tracer (30 day simulation)

- In the tropics: Rapid mixing between surface and tropopause
- Subtropical subsidence region: Low values of tracer mixing ratio
- Midlatitudes-polar regions: Broader mixing
- Quantitative differences between models: FV shows steeper gradient between tropics and subtropics; (day 30) gradient between low and high mixing ratio in subtropics is 2x higher!

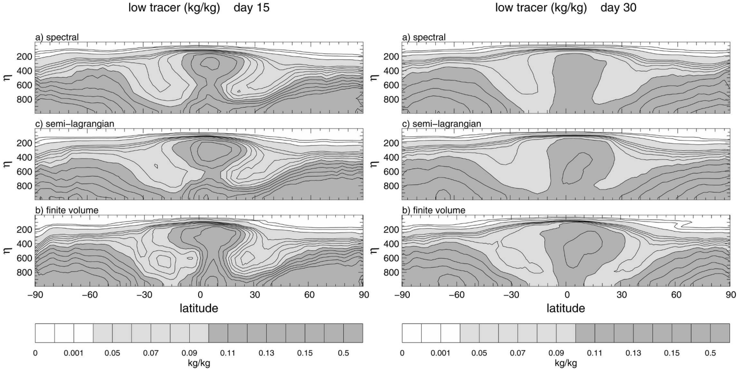

FIG. 2. Zonal averaged mixing ratio for days (left) 15 and (right) 30 for LOW tracer: (a) spectral, (b) semi-Lagrangian, and (c) finite volume.

HIGH tracer (let the model evolve for 30 days):

- Subtropical features seen in LOW tracer also in HIGH tracer
- Substantial differences in mixing in the the upper tropospheric polar region: FV core has preserved initial gradient much more strongly

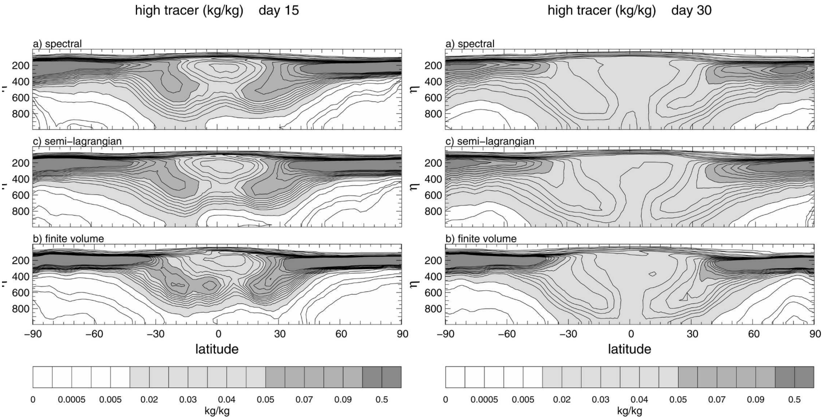

FIG. 3. As in Fig. 2 but for HIGH tracer.

Deep convection

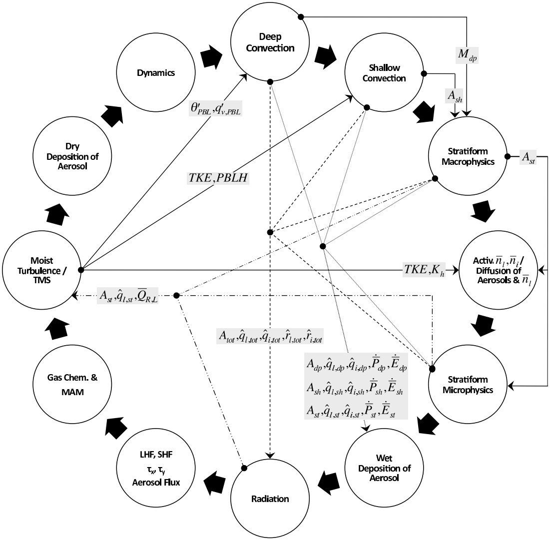

Figure from Park et al. (2012)

Deep convection scheme - schematic (Washington and Parkinson, 2005)

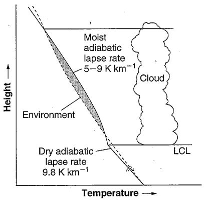

Figure 3.16 Schematic of cumulus cloud formation showing the lifting condensation level (LCL), dry and moist adiabatic lapse rates, and lapse rate for the air outside the cloud (labeled "environment").

Simple model of convective cloud:

(ignoring entrainment, increased buoyancy due to T & q differences between cloud core updrafts and compensating downdrafts outside cloud, ...)

- parcel, say with 50% relative humidity, near surface starts to rise, say from strong heating $\rightarrow$ parcel cools at approximately dry adiabatic lapse rate (9.8 K/km^{-1})
- assume the parcel does not mix (i.e. water vapor content remains the same): **no entrainment**
- as the parcel rises it continues to cool $\rightarrow$ it can hold less water $\rightarrow$ relative humidity increases
- when reaching 100% relative humidity the parcel saturates:
  parcel has reached **Lifting Condensation Level (LCL)**
- from LCL and upward the parcel cools less rapidly (latent heat release of condensation or fusion releases heat): 5-6 K/km^{-1}
- at some point well above LCL the parcel is cooler than the environmental air (stops rising - top of cloud); however, buoyancy forces and the parcels upward momentum can make the cloud extend above the cross-over point.

Consider a model grid cell with area ΔA (typical scale 100km) with several deep convective towers

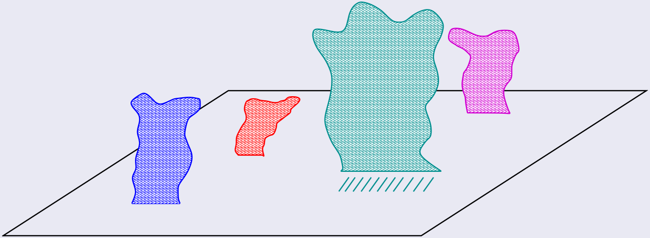

There is a lot going on sub-grid-scale:

- updrafts, downdraft, entrainment, detrainment, condensation, evaporation, ...

What we know is the cell-averaged model state within that grid cell: $(\overline{T}, \overline{q}, \overline{u}, \overline{v}, \overline{P}, ...)$
What the parameterization should give us:

$$\frac{\partial \overline{T}}{\partial t} = \mathcal{F}_T(\overline{T}, \overline{q}, \overline{u}, \overline{v}, \overline{P}, ...) \tag{8}$$

$$\frac{\partial \overline{q}}{\partial t} = \mathcal{F}_q(\overline{T}, \overline{q}, \overline{u}, \overline{v}, \overline{P}, ...) \tag{9}$$

Deep convection scheme - schematic

Ensemble plume approach (Arakawa and Schubert, 1974)

Ensemble of convective updrafts and associated saturated downdrafts exist whenever the atmosphere is conditionally unstable in the lower troposphere $\rightarrow$ effectively the model 'sees' one 'ensemble column' of convection

Among the assumptions are:

- no tilting of the 'ensemble' convective tower
- area of 'ensemble' convective tower $\Delta A_c << \Delta A$ $\rightarrow q_e = \overline{q}$

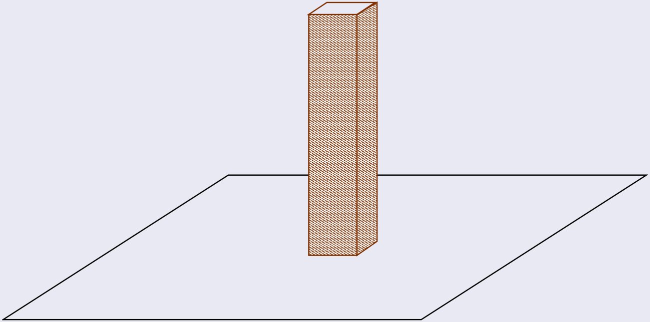

Deep convection scheme - schematic

'Ensemble' convective tower may span many vertical levels (even entire column)

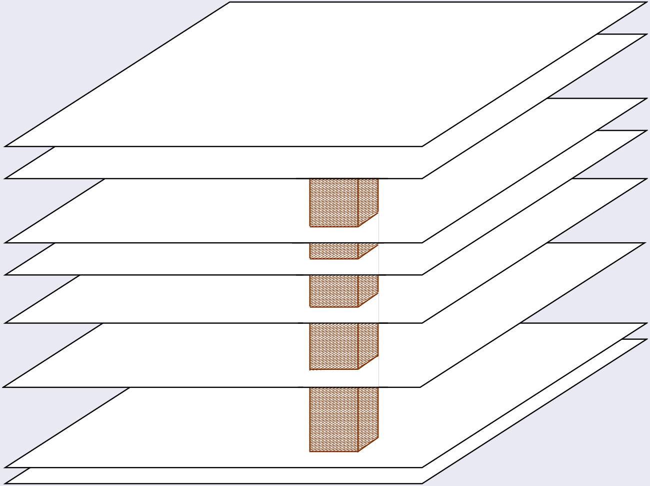

Deep convection scheme - schematic

Consider 'ensemble plume' in one layer:

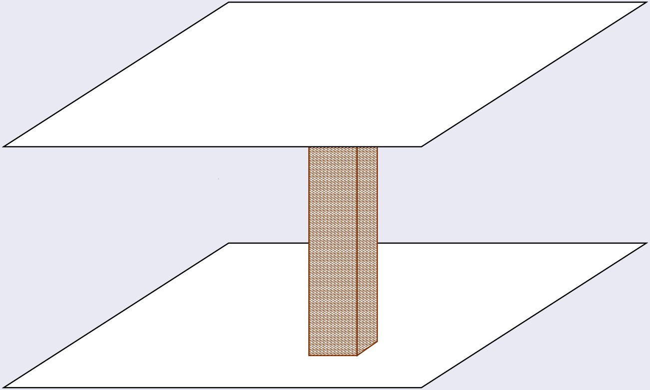

Consider ‘ensemble plume’ in one layer:

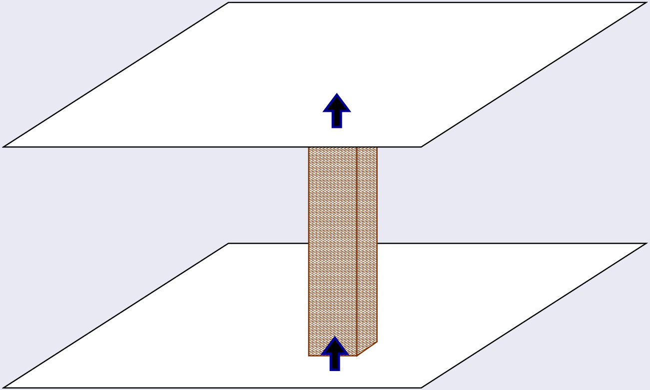

Processes represented:

- M_u: mass flux of ‘ensemble’ updraft defined at model layer interfaces

Deep convection scheme - schematic

Consider 'ensemble plume' in one layer:

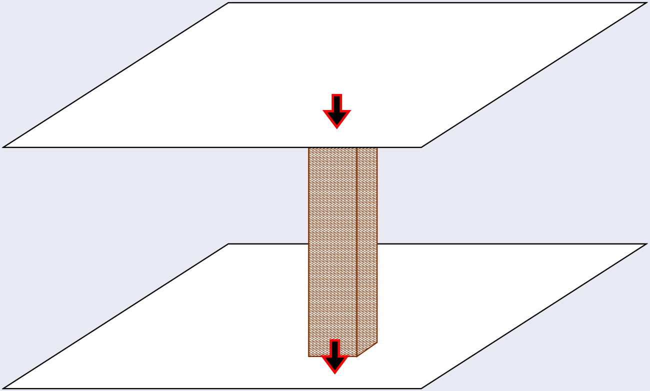

Processes represented:

- M_u: mass flux of 'ensemble' updraft defined at model layer interfaces
- M_d: mass flux of 'ensemble' downdraft defined at model layer interfaces

Consider 'ensemble plume' in one layer:

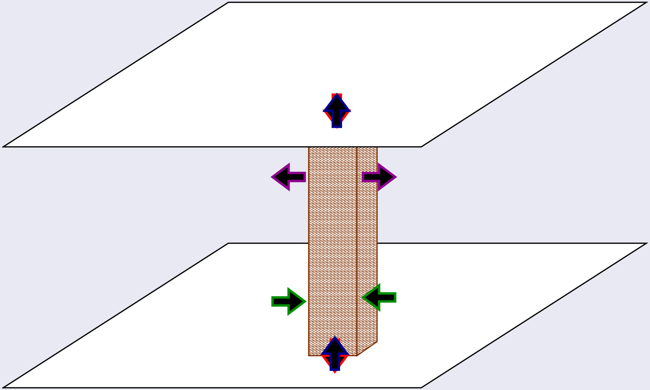

Processes represented:

- M_u: mass flux of 'ensemble' updraft defined at model layer interfaces
- M_d: mass flux of 'ensemble' downdraft defined at model layer interfaces
- E_x, $x = u, d$: entrainment rate of environmental air associated with updrafts and downdrafts, respectively (defined at layer centers)

Deep convection scheme - schematic

Consider 'ensemble plume' in one layer:

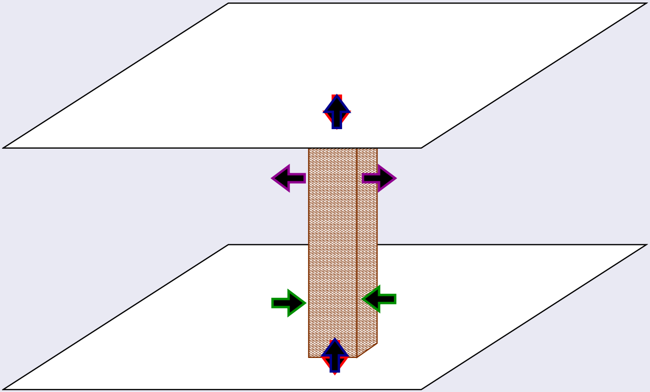

Processes represented:

- M_u: mass flux of 'ensemble' updraft defined at model layer interfaces
- M_d: mass flux of 'ensemble' downdraft defined at model layer interfaces
- E_x, $x = u, d$: entrainment rate of environmental air associated with updrafts and downdrafts, respectively (defined at layer centers)
- D_x, $x = u, d$: detrainment rate of 'plume air' associated with updrafts and downdrafts, respectively

Deep convection scheme - schematic

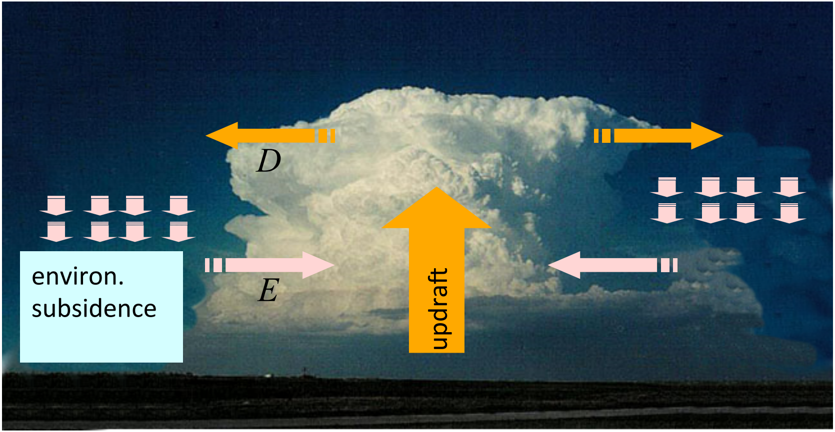

Figure courtesy of J. Bacmeister (NCAR)

Deep convection scheme - schematic

CAM5 deep convection scheme

The challenge of cloud researchers is to determine how nature decides which process dominates under different large-scale environmental conditions.

 

CAM5 deep convection scheme is a simplification of Arakawa and Schubert (1974) for large-scale models (Zhang and McFarlane, 1995) with modified momentum transport by Richter and Rasch (2008) and a modified dilute plume calculation following Raymond and Blyth (1992)

The details of how the deep convection scheme determines M_u, M_d, E_u, D_u, E_d, E_u is beyond the scope of this talk (local experts: S. Park, R. Neale, J. Bacmeister), i.e. assume that mass-fluxes, entrainment and detrainment rates are given!

Deep convective tracer transport

Convection is an effective way of mixing tracers in the vertical (e.g. Mahowald et al., 1995; Collins et al., 1999), e.g., convective updrafts can transport a tracer from the surface to the upper troposphere on time scales of $\mathcal{O}(1h)$.

Steady state continuity equation for 'bulk' updraft mixing ratio φ_u

$$\frac{\partial\left(M_u\varphi_u\right)}{\partial p} = E_u\varphi_e - D_u\varphi_u \tag{8}$$

where

- M_u is mass-flux at layer interfaces
- φ_e mixing ratio of environment (in CAM: $\varphi_e = \overline{\varphi}$; i.e. we assume that area of updraft << grid cell area)
- E_u and D_u are entrainment/detraiment rates for the updrafts.

Solve (8) for φ_u

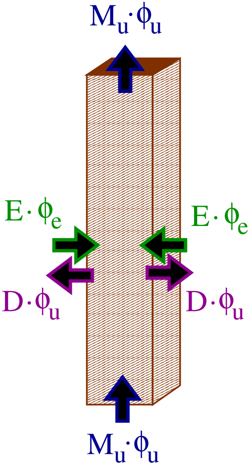

CAM5 subroutine convtran in physics/cam/zm_conv.F90 file

Convection is an effective way of mixing tracers in the vertical (e.g. Mahowald et al., 1995; Collins et al., 1999), e.g., convective updrafts can transport a tracer from the surface to the upper troposphere on time scales of $\mathcal{O}(1h)$.

Steady state continuity equation for 'bulk' downdraft mixing ratio φ_d

$$\frac{\partial \left(M_d \varphi_d\right)}{\partial p} = E_d \varphi_e - D_d \varphi_d \tag{8}$$

where

- M_d is mass-flux at layer interfaces
- φ_e mixing ratio of environment (in CAM: $\varphi_e = \overline{\varphi}$; i.e. we assume that area of updraft $<<$ grid cell area)
- E_d and D_d are entrainment/detraiment rates for the downdrafts.

Solve (8) for φ_d

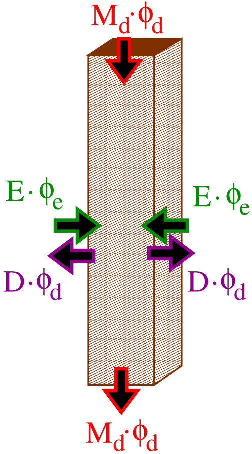

CAM5 subroutine convtran in physics/cam/zm_conv.F90 file

Convection is an effective way of mixing tracers in the vertical (e.g. Mahowald et al., 1995; Collins et al., 1999), e.g., convective updrafts can transport a tracer from the surface to the upper troposphere on time scales of $\mathcal{O}(1h)$.

Steady state continuity equation for 'bulk' downdraft mixing ratio φ_d

$$\frac{\partial \left(M_d \varphi_d\right)}{\partial p} = E_d \varphi_e - D_d \varphi_d \tag{8}$$

where

- M_d is mass-flux at layer interfaces
- φ_e mixing ratio of environment (in CAM: $\varphi_e = \overline{\varphi}$; i.e. we assume that area of updraft $<<$ grid cell area)
- E_d and D_d are entrainment/detrainment rates for the downdrafts.

Solve (8) for φ_d

$$\frac{\partial \overline{\varphi}}{\partial t} = \frac{\partial}{\partial p}\left[M_u \left(\varphi_u - \overline{\varphi}\right) + M_d \left(\varphi_d - \overline{\varphi}\right)\right] \tag{9}$$

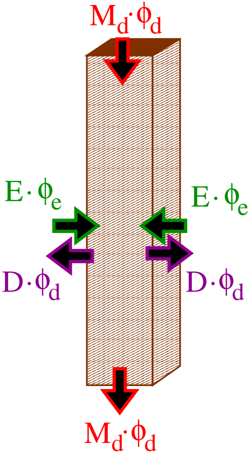

CAM5 subroutine convtran in physics/cam/zm_conv.F90 file

How much mixing does deep convection do?

Use Rasch et al. (2006) transport test setup: day 0 , zonal average

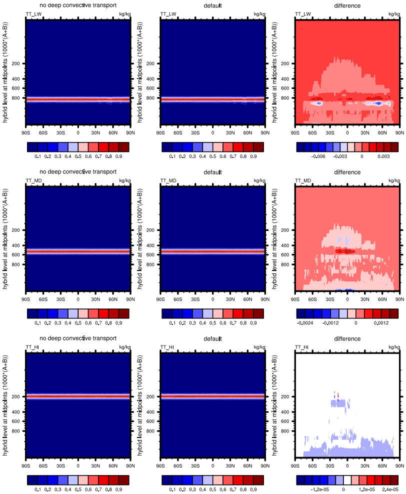

(left) no deep convective transport of tracers - there is deep convective transport of water variables!, (middle) default, (right) difference

Use Rasch et al. (2006) transport test setup: day 1 , zonal average

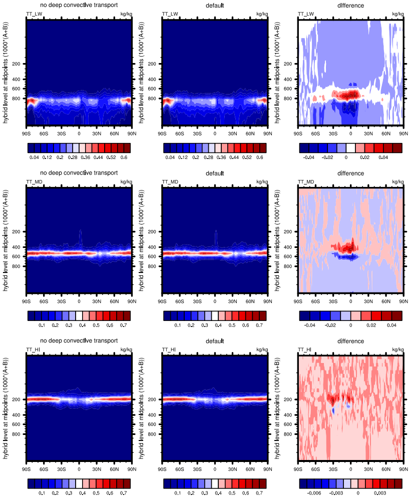

(left) no deep convective transport of tracers - there is deep convective transport of water variables!, (middle) default, (right) difference

Use Rasch et al. (2006) transport test setup: day 5 , zonal average

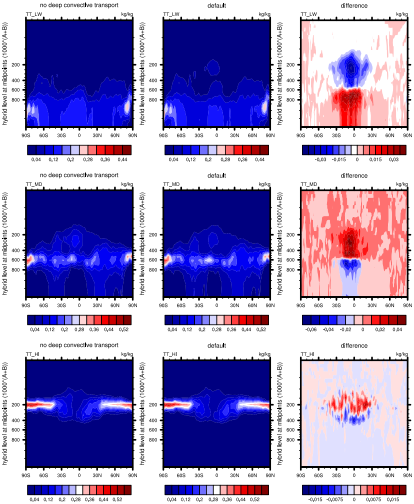

(left) no deep convective transport of tracers - there is deep convective transport of water variables!, (middle) default, (right) difference

How much mixing does deep convection do?

Use Rasch et al. (2006) transport test setup: day 1 , along Equator

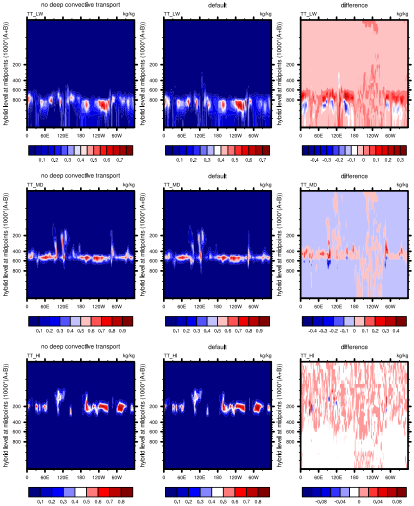

(left) no deep convective transport of tracers - there is deep convective transport of water variables!, (middle) default, (right) difference

Shallow convection

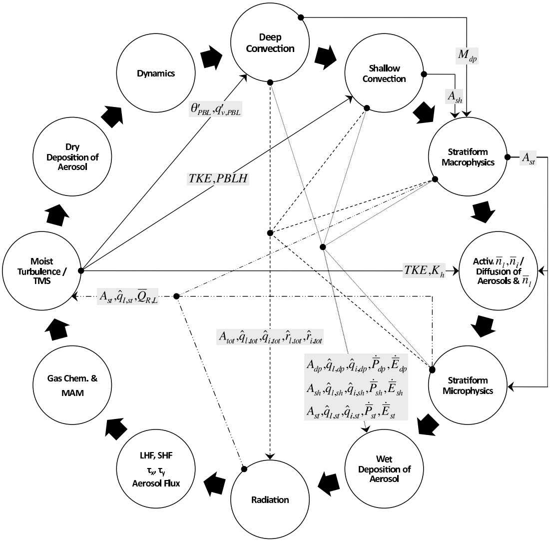

Figure from Park et al. (2012)

Turbulent mixing

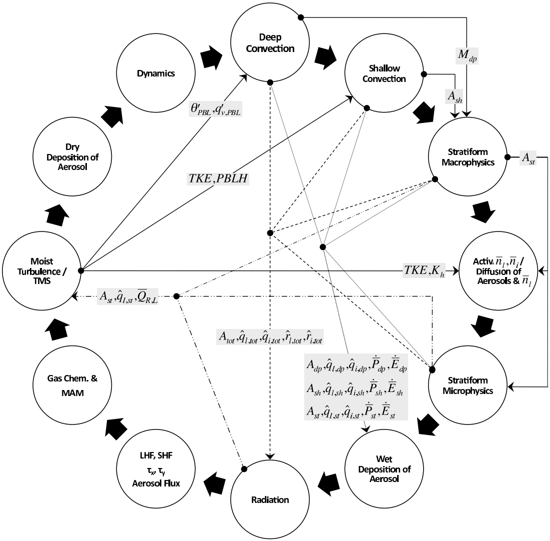

Figure from Park et al. (2012)

Turbulent diffusion

Given vertical profile of eddy diffusion coefficient $K(p)$:

$$\frac{\partial \overline{\varphi}}{\partial t} = \frac{\partial}{\partial p}\left[K(p)\frac{\partial \overline{\varphi}}{\partial p}\right] \tag{10}$$

Contrary to convective tracer transport turbulent diffusion is a local process!

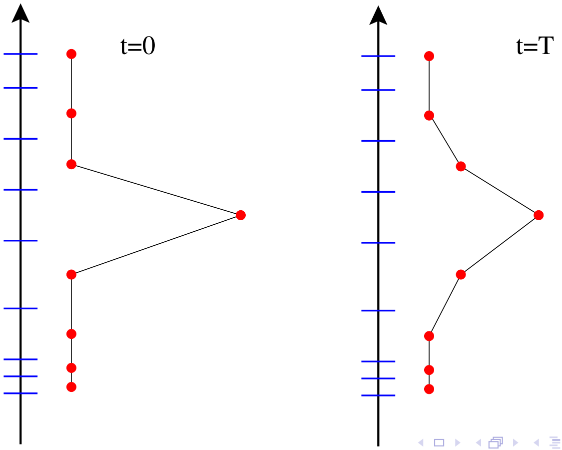

This completes the 'cycle'

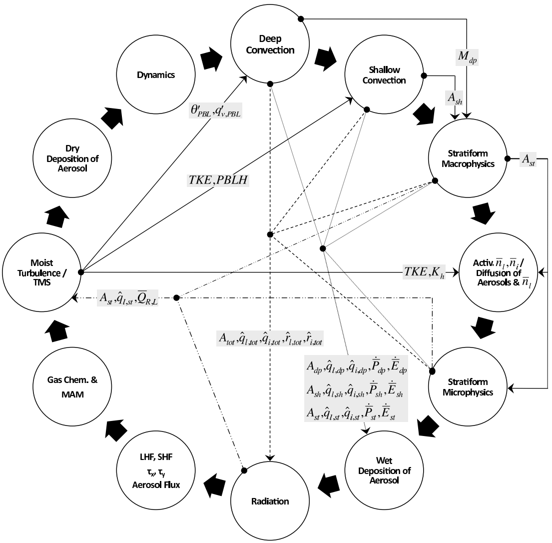

Figure from Park et al. (2012)

References I

Arakawa, A. and Schubert, W. H. (1974). Interaction of a cumulus cloud ensemble with the large-scale environment, Part I. *J. Atmos. Sci.*, 31:674–701.

Colella, P. and Woodward, P. R. (1984). The piecewise parabolic method (PPM) for gas-dynamical simulations. *J. Comput. Phys.*, 54:174–201.

Collins, W., Stevenson, D. S., Johnson, C., and Derwent, R. G. (1999). Role of convection in determining the budget of odd hydrogen in the upper troposphere. *J. Geophys. Res.*, 104:26 927–26 941.

Lauritzen, P. and Thuburn, J. (2012). Evaluating advection/transport schemes using interrelated tracers, scatter plots and numerical mixing diagnostics. *Quart. J. Roy. Met. Soc.*, 138(665):906–918.

Lauritzen, P. H. (2007). A stability analysis of finite-volume advection schemes permitting long time steps. *Mon. Wea. Rev.*, 135:2658–2673.

Lauritzen, P. H., Skamarock, W. C., Prather, M. J., and Taylor, M. A. (2012). A standard test case suite for 2d linear transport on the sphere. *Geo. Geosci. Model Dev. Discuss.*, 5:189–228.

Lin, S. J. and Rood, R. B. (1996). Multidimensional flux-form semi-Lagrangian transport schemes. *Mon. Wea. Rev.*, 124:2046–2070.

Machenhauer, B., Kaas, E., and Lauritzen, P. H. (2009). Finite volume methods in meteorology, in: R. Temam, J. Tribbia, P. Ciarlet (Eds.), Computational methods for the atmosphere and the oceans. *Handbook of Numerical Analysis*, 14. Elsevier, 2009, pp.3-120.

Mahowald, N., Rasch, P. J., and Prinn, R. G. (1995). Cumulus parameterizations in chemical transport models. *J. Geophys. Res.*, 100:26 173–26 189.

Nair, R. D., Levy, M. N., and Lauritzen, P. H. (2011). Emerging numerical methods for atmospheric modeling, in: P.H. Lauritzen, R.D. Nair, C. Jablonowski, M. Taylor (Eds.), Numerical techniques for global atmospheric models. *Lecture Notes in Computational Science and Engineering, Springer*, 80.

Neale, R. B., Richter, J. H., and Jochum, M. (2008). The impact of convection on ENSO: From a delayed oscillator to a series of events. *J. Climate*, 21:5904–5924.

Park, S. and Bretherton, C. S. (2009). The university of washington shallow convection and moist turbulence schemes and their impact on climate simulations with the community atmosphere model. *J. Climate*, 22:3449–3469.

Park, S., Bretherton, C. S., and Rasch, P. J. (2012). Global cloud simulation in the community atmosphere model, 5. *J. Climate*. in prep.

Rasch, P. J., Coleman, D. B., Mahowald, N., Williamson, D. L., Lin, S. J., Boville, B. A., and Hess, P. (2006). Characteristics of atmospheric transport using three numerical formulations for atmospheric dynamics in a single GCM framework. *J. Climate*, 19:2243–2266.

Raymond, D. and Blyth, A. (1992). Extension of the stochastic mixing model to cumulonimbus clouds. *J. Atmos. Sci.*, 49(21):1968–1983.

Richter, J. H. and Rasch, P. J. (2008). Effects of convective momentum transport on the atmospheric circulation in the community atmosphere model, version 3. *J. Climate*, 21(7):1487–1499.

van Leer, B. (1977). Towards the ultimate conservative difference scheme. IV: A new approach to numerical convection. *J. Comput. Phys.*, 23:276–299.

Washington, W. M. and Parkinson, C. L. (2005). *Introduction To Three-dimensional Climate Modeling*. University Science Books.

Zhang, G. and McFarlane, N. (1995). Sensitivity of climate simulations to the parameterization of cumulus convection in the canadian climate center general-circulation model. *ATMOSPHERE-OCEAN*, 33(3):407–446.